View metadata, citation and similar papers at core.ac.uk

brought to you by CORE

Paper

Frequency Offset Compensation for OFDM Systems Using a Combined Autocorrelation and Wiener Filtering Scheme

Ali Ramadan Ali, Tariq Jamil Khanzada, and Abbas Omar

Abstract—One of the orthogonal frequency division multiplexing (OFDM) system disadvantages is its sensitivity to frequency offset and phase noise, which lead to losing the orthogonality between the subcarriers and thereby degrade the system performance. In this paper a joint scheme for frequency offset and pilot-based channel estimation is introduced in which the frequency offset is first estimated using an autocorrelation method, and then is fined further by applying an iterative phase correction by means of pilot-based Wiener filtering method. In order to verify the capability of the estimation algorithm, the scheme has been implemented and tested using a real measurement system in a multipath indoor environment. The results show the algorithm capability of compensating for the frequency offset with different transmission and channel conditions.

Keywords—channel characterization, frequency offset, OFDM measurement, Wiener filtering.

1. Introduction

Orthogonal frequency division multiplexing (OFDM) divides the base bandwidth into N orthogonal narrow subchannels transmitted in parallel. The generation of the OFDM signals at the transmitter is accomplished using inverse fast Fourier transform (IFFT), which delivers orthogonal carriers. Due to its long symbol duration together with adding a suitable guard interval (GI) to the time domain signal, OFDM system can handel the frequency selective fading resulting from the multipath effect. The source bit stream in OFDM system is first encoded, interleaved and then mapped using a common modulation scheme like quadrature amplitude modulation (QAM) or phase shift keying (PSK).

The resulting symbols are arranged in blocks with length N, and then IFFT is applied, so that, each symbol is given an orthogonal carrier. In order to cope with the multipath effect a suitable GI (longer than the channel impulse response) is inserted in the time domain signal before transmission. In OFDM system usually a so called cyclic prefix GI is used, which inserts the last portion of the OFDM symbol at the beginning. This type of GI allows for circular convolution with the channel and maintains the orthogonality of the carriers. The ability of combating the frequency selective channels has resulted in choosing the OFDM system as a standard modulation scheme for transmitting high rate services as in IEEE 802.11a/g wireless local area network (WLAN) [1], digital audio broadcasting DAB [2], digital video broadcasting (DVB) [3], and became a promising candidate for fourth generation (4G) mobile communication systems [4], [5]. On the other hand OFDM is sensitive to phase noise and frequency offsets, which cause phase rotation and loss in the orthogonality between the subcarriers.

This introduces intercarrier interference (ICI) [6]–[9] as another source of noise, which degrades the system performance. The notation to be adopted throughout this paper conforms to the following convention: bold uppercase letters $\mathbf{H}$ denote matrices, bold uppercase underlined letters $\underline{\mathbf{V}}$ denote frequency domain vectors, while time domain vectors are represented by bold lowercase underlined letters $\underline{\mathbf{v}}$, variables in time are denoted by lowercase letters $v(n)$, and in frequency by uppercase letters $V(n)$. The operator $\{.\}^H$, represents Hermitian transpose. $\mathbf{I}$ denotes the identity matrix.

2. System Model and the Measurement Setup

Making use of the FFT operation, the time domain transmitted OFDM symbol can be written as [10]

$$x(n) = \sum_{m=0}^{N-1} S(m) \mathrm{e}^{\mathrm{j}\frac{2\pi nm}{N}} \qquad 0 \le n \le N-1\,, \tag{1}$$

where $S(m)$ is the QAM symbol at the mth subcarrier. Because of the cyclic prefix, the transmitted signal is circularly convolved with the impulse response of the multipath time-variant channel. The received time domain OFDM symbol is expressed as

$$y(n) = \sum_{l=0}^{L-1} h(n,l)x(n-\tau_l) + v(n), \tag{2}$$

where $h(n,l)$ and τ_l are the complex random variable and the corresponding tap delay, respectively, at the lth path of the multipath channel, and $v(n)$ represents the additive white Gaussian noise at sample instant n. After applying FFT at the receiver side, the frequency domain OFDM symbol becomes

$$Y(k) = \frac{1}{N} \sum_{n=0}^{N-1} \Big(\sum_{l=0}^{L-1} h(n,l)x(n-\tau_l) + v(n) \Big) \mathrm{e}^{-\mathrm{j}\frac{2\pi nk}{N}}\,. \tag{3}$$

Equation (3) can be simplified [9] to

$$Y(k) = S(k)H_{k,k} + \underbrace{\sum_{m \neq k} S(m)H_{k,m}}_{\text{ICI}} + V(k), \tag{4}$$

where:

$$H_{k,m} = \frac{1}{N} \sum_{n=0}^{N-1} \sum_{l=0}^{L-1} h(n,l) \mathrm{e}^{-\mathrm{j}\frac{2\pi}{N}(k(\tau_l - n)+nk)}. \tag{5}$$

Writing (4) in vector form representation gives

$$\underline{\mathbf{Y}} = \mathbf{H}\underline{\mathbf{S}} + \underline{\mathbf{V}}, \tag{6}$$

thus the main diagonal of the matrix **H** represents the channel response at the subcarriers, while the off-diagonals represent the ICI components result from the frequency offsets and the time variation of the channel.

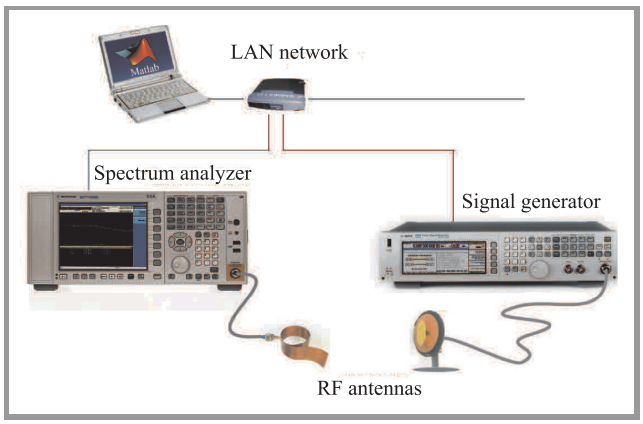

Fig. 1. The measurement system setup.

The measurement setup of the OFDM system is shown in Fig. 1. As shown from the figure, the measurement system is a combination of software and hardware components.

2.1. Software Setup

At an external PC, the baseband IQ (in-phase and quadrature-phase) OFDM signal based on IEEE 802.11g standard is generated using Matlab code. The OFDM symbols are arranged in a few frames to be transmitted. At the beginning of each frame, some training symbols (preambles) are inserted, which are used for packet detection and frequency and time offset estimation. The time domain baseband signal is sent via LAN connection to the transmitter, in order to be up-converted and transmitted through the wireless channel. The commands for controlling the power and the carrier frequency are sent to the transmitter before sending the baseband signal. On the other hand, the IQ data from the captured signal at the receiver is sent back to the external PC via the LAN for processing. Packet detection, frequency and time offset estimation and pilot-based channel estimation are all accomplished using Matlab.

2.2. Hardware Setup

2.2.1. The Transmitter

For transmitting the real time multicarrier signal, an MXG signal generator N5182A [11] has been used. This signal generator works on a frequency range between 100 kHz to 6 GHz and transmission power up to 17 dBm. The baseband IQ data is generated using Matlab and sent to the signal generator via LAN connection. The signal generator saves the IQ data, applies the IF modulation and RF upconversion and then transmits the signal with predefined power and carrier frequency. In order to have a continuous transmission, the signal generator sends the same signal repeatedly.

2.2.2. The Antennas

The transmit antenna works between 2.4 GHz and 2.6 GHz with gain 9 dBi at the resonance frequency [12], while the receive antenna has an ultra-wideband characteristics in the frequency range from 800 MHz to 18 GHz [13]. Both antennas have been fabricated in the Institute of Electronics, Signal Processing and Communications (IESK) at the Otto von Guericke University of Magdeburg, Germany.

2.2.3. The Receiver

The EXA spectrum analyzer from Agilent [14] has been used as a receiver. This device has an absolute sensitivity of −79.4 dBm, a dynamic range of 93.1 dB, and a maximum input power of +30 dBm. The reviver down converts the RF signal and generates the IQ baseband data which is sent back to the external PC for processing.

3. Wireless Channel Characterization

Estimating the channel parameters such as the number of multipaths, the delay spread, and the Doppler spread allows for suitable design and robust behavior of the system. In this section some measurements have been made in order to estimate the channel taps and the delay spread of the channel. An OFDM signal has been sent through the channel, captured at the receiver and then processed in order to calculate the channel transfer function (CTF) and the channel impulse response (CIR). The measurements have been conducted in Lab312, which is one of the IESK laboratories at the University of Magdeburg. The lab was clustered with furniture, test and measurement equipments. The topology of the lab and the test scenario is shown in Fig. 2.
During the measurements, the transmit antenna remained fixed at the same place with different orientations, while the receive antenna was moved to different places and orientations. The signal used for measurement was a WLAN signal with 20 MHz bandwidth and carrier frequency of 2.412 GHz. The channel transfer function was calculated as the ratio between the transmitted frequency domain OFDM symbols by the received frequency domain

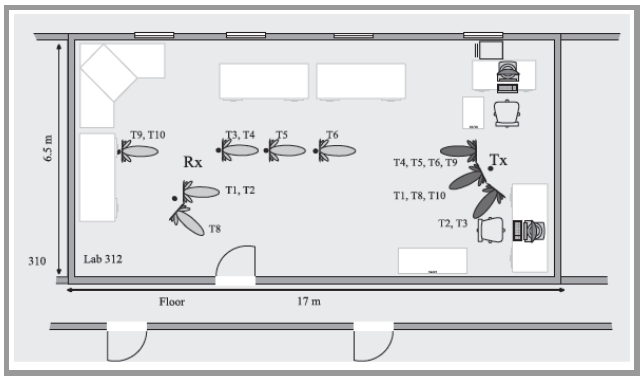

Fig. 2. The floor plan of the measurement location.

symbols. The channel impulse response h was calculated by simply applying an IFFT on the CTF.

One of the important parameters required for the characterization of any wireless channel is the root mean square delay spread τ_{rms}, which is calculated from the CIR [15] as

$$\tau_{rms} = \sqrt{\frac{\sum_{l=0}^{L-1} h_l^2 \tau_l^2}{\sum_{l=0}^{L-1} h_l^2} - \left(\frac{\sum_{l=0}^{L-1} h_l^2 \tau_l}{\sum_{l=0}^{L-1} h_l^2} \right)^2}. \tag{7}$$

In order to get a clear idea about the multipath channel, the Ricean K-factor of the channel has also been calculated by taking the ratio between the signal power in the main path to the power in the scattered paths as follows:

$$K = \frac{h_{LOS}^2}{\sum_{l=0}^{L-1} h_l^2 - h_{LOS}^2}. \tag{8}$$

Basically, the Ricean K factor lies between 0, in case of Rayleigh channel, and ∞ in the case of single path transmission. The measured channel parameters are summarized in Table 1.

Table 1

The measured channel characteristics

Test	Delay spread τ_{rms} [ns]	K factor [dB]	C_f [kHz]
T1	306.3	8.8195	653
T2	236	5.7749	847
T3	138	10.5308	1449
T4	97	10.8814	2062
T5	61	11.2222	3279
T6	58	11.3988	3448
T7	143	9.0309	1399
T8	233	10.2531	858
T9	151	10.8991	1325
T10	183	10.5308	1093

In addition, the coherence bandwidth of the channel has been approximately calculated according to the 50% of the frequency correlation function [15] as

$$C_f \approx \frac{1}{5\tau_{rms}}. \tag{9}$$

The measured parameters show that τ_{rms} lies between 306 ns and 58 ns for different locations. Figure 3 shows

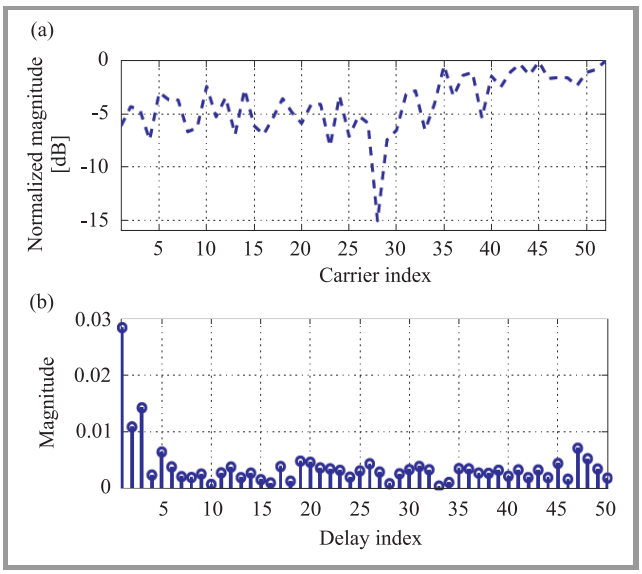

Fig. 3. The CTF (a) and the CIR (b) of a multipath channel (T1).

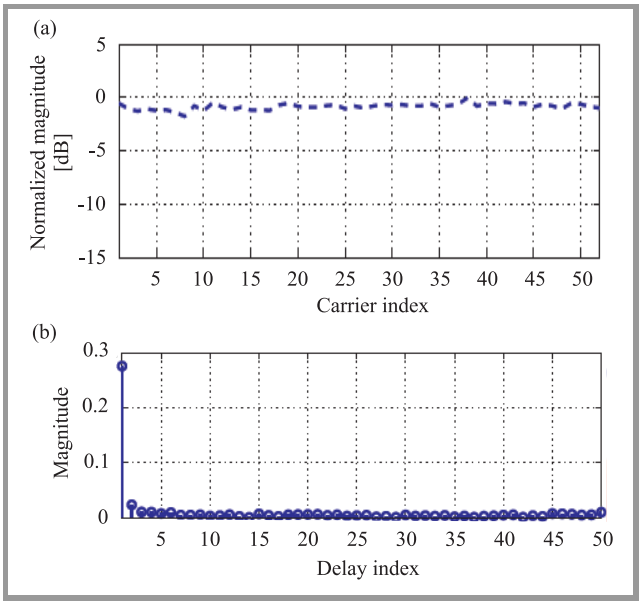

Fig. 4. The CTF (a) and the CIR (b) of a flat fading channel (T5).

the CTF and the CIR of the experiment T1, which represents a multipath channel with $\tau_{rms} = 306$ ns, while Fig. 4 represents the experiment T5, which exhibits a strong line of sight (LOS) transmission.

4. A Joint Frequency Offset and Wiener Filtering Channel Estimation Scheme

The time and frequency synchronization play an important role in designing and implementing the practical systems. In WLAN system, the signal is headed with a preamble at the beginning of each frame. This preamble is basically used for time synchronization, frequency offset estimation and for the initial channel estimation. The preamble contains two parts, the first one is called short training symbols (STS), which contains 10 short symbols occupy 8 μs. The STS are used for time synchronization and course frequency offset (CFO) estimation. The second part is called long training symbols (LTS), which contains two long symbols each with time duration of 3.2 μs as well as a GI with time duration of 1.6 μs. The LTS are used for further enhancing the time synchronization and for fine frequency offset (FFO) estimation as well as initial channel estimation.

The OFDM symbol of the WLAN system contains 64 carriers, 52 of them are active carriers, while the other 12 carriers work as frequency guard at both sides of the spectrum. For channel estimation and equalization proposes, 4 carriers out of the 52 are booked for pilots.

In order to start processing the received OFDM signal, the signal packets need to be detected first and the first sample of the OFDM symbols needs to be indicated in order to apply the FFT operation on the right symbol samples. A suitable method for detecting the packet is based on the autocorrelation of the received preamble [16], which contains short and long training symbols. The auto correlation is written in the following form

$$Z(n) = \sum_{c=0}^{N_{TS}-1} y^*(n+c)y(n+c+N_{TS}), \tag{10}$$

where $y(n)$ represents the nth incoming sample of the baseband signal, $y^*(n)$ represents the conjugate of $y(n)$ and $N_{TS} = 16$ samples in case of short training symbols. In order to avoid the expected variance of the incoming signal power, the autocorrelation needs to be normalized by a moving sum of the received signal power [17]. The moving sum of the received power can be written as

$$P(n) = \sum_{c=0}^{N_{TS}-1} |y(n+c+N_{TS})|^2. \tag{11}$$

The normalized autocorrelation used for packet detection reads

$$M(n) = \frac{|Z(n)|^2}{P(n)}. \tag{12}$$

The packet is detected at the first peak of $M(n)$ after a predefined threshold, which should be chosen to minimize the possibility of false alarm. Using only the short training symbols in packet detection gives a reasonable performance in case of good conditions of the channel, however, because of the expected time offsets at bad channel conditions, it is better to use both short and long training symbols for this purpose.

Figure 5 shows the autocorrelation function $M(n)$, whose first peak indicates the beginning of the packet (the first sample of the short training symbols), while the second peak indicates the first sample of the GI of the long training symbols. By taking the difference between the two peaks, the time offset, if found, can be estimated and then the start of the packet is corrected.

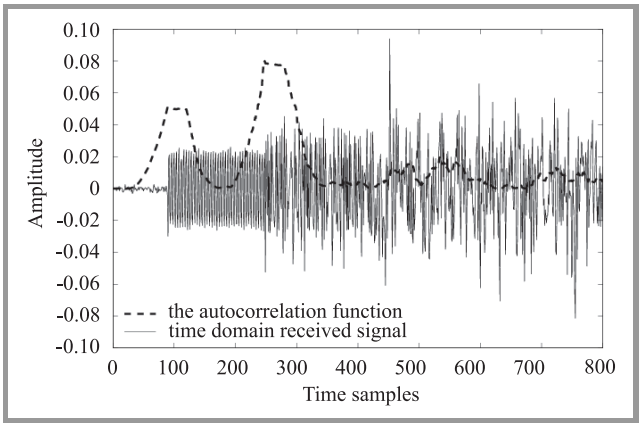

Fig. 5. The packet detection based on autocorrelation of the preamble.

Figure 6 presents a comparison between the spectrum of the transmitted and the received OFDM signals. The figure shows the effect of the widowing at the receiver side, which reduces the side loops of the spectrum.

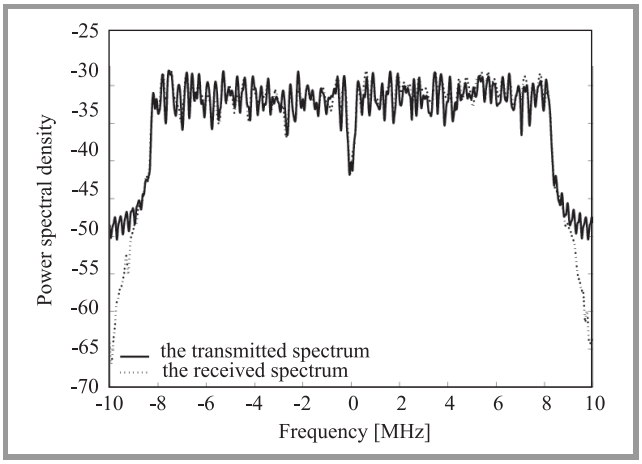

Fig. 6. A comparision between the transmitted and measured spectrum of the OFDM signal.

As a consequence of the frequency offsets between the oscillators of the transmitter and the receiver, phase errors and ICI occur on the received signal and lead to degrading the OFDM system performance. The frequency offset can be estimated from the autocorrelation of the training symbols in the preamble. If there is a frequency offset f_e,

the autocorrelation function will be modified by the phase error as

$$Z(n) = \mathrm{e}^{-\mathrm{j}2\pi f_e N_{TS}} \sum_{c=0}^{N_{TS}-1} |y(n+c)|^2. \tag{13}$$

The phase introduced by the frequency offset is calculated as

$$\phi = \angle Z(n).$$

The course frequency offset CFO is calculated in case of the short symbols as

$$f_e = \frac{\phi}{2\pi 16T}, \tag{14}$$

where T is the sampling time which is (50 ns) for WLAN system. For better frequency offset estimation, the estimation is accomplished in two stages CFO and then FFO estimations. After the compensation of the frequency offset, a Wiener filtering method described is applied to further correcting for the phase rotation, and at the same time equalizing the OFDM symbols. In order to enhance the performance of the frequency offset compensation, a minimum mean square error (MMSE) [18]–[20] estimator based on Wiener filtering has been used. The frequency domain MMSE estimator minimizes the following formula:

$$E\{|e|^2\} = E\{|\underline{\mathbf{H}}_p - \underline{\widehat{\mathbf{H}}}_p|^2\}.$$

The frequency domain channel matrix can be estimated by linearly filtering the received signal for each channel element. The estimated element (m,k) of the channel matrix is expressed as follows:

$$\hat{H}_{m,k} = \underline{\mathbf{W}}_{m,k}^H \underline{\mathbf{Y}}, \tag{15}$$

where $\underline{\mathbf{W}}_{m,k}$ is the Wiener filter vector that is used to estimate the channel matrix element (m,k).
The Wiener filter for each channel element is designed and optimized according to the MMSE criterion as follows:

$$\underline{\mathbf{W}}_{m,k}^{(opt)} = \arg \min_{\underline{\mathbf{W}}} E\left\{\left|H_{m,k} - \underline{\mathbf{W}}_{m,k}^H \underline{\mathbf{Y}}\right|^2\right\}. \tag{16}$$

The solution of Eq. (16) is given by [21]

$$\underline{\mathbf{W}}_{m,k}^{(opt)} = \mathbf{R}^{-1} \underline{\mathbf{P}}_{m,k}, \tag{17}$$

where $\mathbf{R} = E\{\underline{\mathbf{Y}}\underline{\mathbf{Y}}^H\}$ is the autocorrelation of the received frequency domain signal and $\underline{\mathbf{P}}_{m,k} = E\{H_{m,k}^* \underline{\mathbf{Y}}\}$ is the cross correlation between the received signal and the actual frequency response of the channel. The derivation of these correlation matrices is detailed in Appendix.
In order to correct the phase rotation of the captured OFDM symbols, an iterative scheme is applied to find the phase error that minimizes the following cost function:

$$MSE = E\{|\underline{\mathbf{S}}_p - \underline{\hat{\mathbf{S}}}_p|^2\}, \tag{18}$$

where $\underline{\mathbf{S}}_p$ and $\underline{\hat{\mathbf{S}}}_p$ are vectors contain the transmitted and equalized pilots.

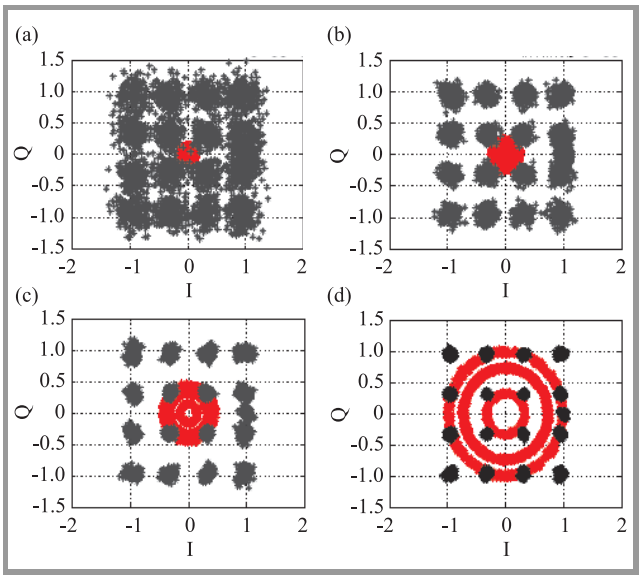

Fig. 7. The constellation of the equalized 16 QAM modulated OFDM symbols with different transmission power: (a) 0 dBm, (b) 5 dBm, (c) 10 dBm, (d) 17 dBm at distance ($d = 2$ m); gray: received symbols, black: equalized symbols.

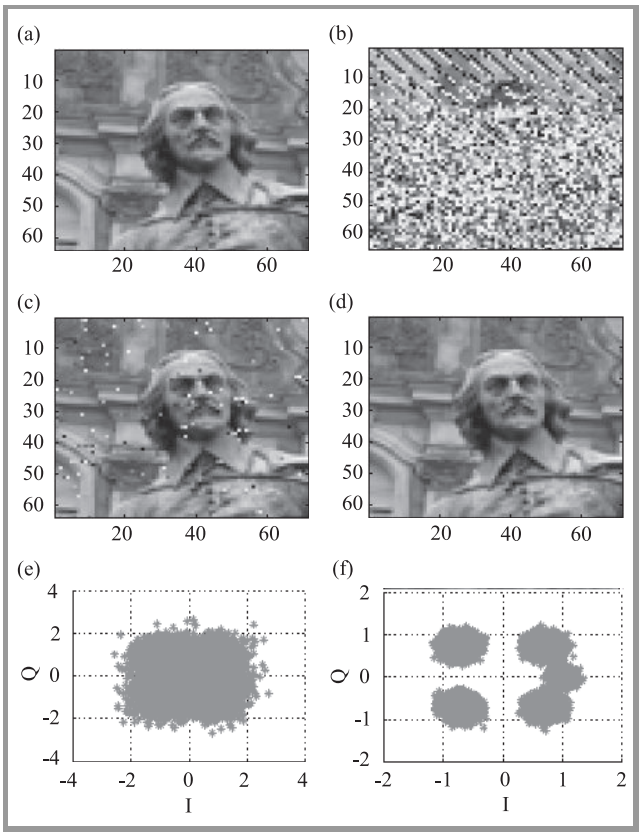

Fig. 8. An example of transmitting a gray scaled image through the wireless channel: (a) the transmitted image; (b) the received un-equalized image; (c) the equalized image with a transmission power -10 dBm; (d) the equalized image with a transmission power 0 dBm; (e) the constellation of the equalized image with -10 dBm power; (f) the constellation of the equalized image with 0 dBm power.

$\underline{\hat{\mathbf{S}}}_p$ is estimated using LS criterion as follows:

$$\underline{\hat{\mathbf{S}}}_p = \mathcal{D}(\underline{\hat{\mathbf{H}}}_p)^{-1}\underline{\mathbf{Y}}_p, \tag{19}$$

where $\underline{\mathbf{Y}}_p$ is the received pilots, $\mathcal{D}(\cdot)$ is vector to diagonal matrix conversion, and $\underline{\hat{\mathbf{H}}}_p$ is the estimated CTF, which is estimated by Wiener filtering of the received signal as follows:

$$\hat{H}_p = (\mathbf{R}_p^{-1}\underline{\mathbf{P}}_p)^H\underline{\mathbf{Y}}_p. \tag{20}$$

According to Eqs. (24) and (25), the autocorrelation $\mathbf{R}_p$ and the cross-correlation $\underline{\mathbf{P}}_p$ contain information about the delay τ_l of each channel tap. In order to correct the phase rotation, the scheme is searching for τ_0 that minimizes Eq. (18), and then applied the resulting filter for channel equalization.

Figure 7 illustrates the constellation of the equalized 16 QAM modulated OFDM symbols with different transmitted power. For simplicity, we used pilot carriers with the same magnitude.

Figure 8 shows an example of transmitting and receiving a gray scaled image through the wireless channel. The size of the image was 5.4 KB, which required 756 OFDM symbols coded by a convolutional encoder with coding rate of $R = 0.5$.

Table 2 and Fig. 9 represent the measured BER and MSE for different transmission power using 16 QAM modulation scheme for antenna separation of 2 m.

Table 2
The measured system performance with 16 QAM modulation scheme

Transmission power [dBm]	MSE [dB]	BER
–10	–5.5000	0.213
–5	–10.0000	0.0771
0	–14.5000	0.0093
5	–18.9500	$2.5431 \cdot 10^{-5}$
10	–23.5000	0

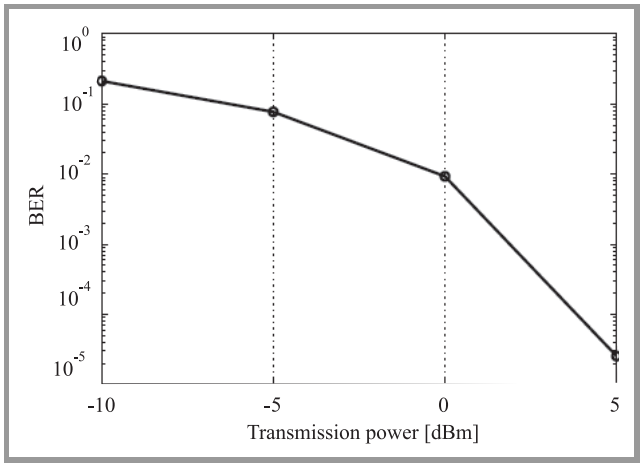

Fig. 9. The measured BER versus the transmission power with modulation scheme 16 QAM at distance ($d = 2$ m).

Table 3 and Fig. 10 represent the measured BER and MSE for different transmission power using 4 QAM modulation scheme for antenna separation of 2 m.

Table 3
The measured system performance with 4 QAM modulation scheme

Transmission power [dBm]	MSE [dB]	BER
–5	–11.5	$2.84 \cdot 10^{-4}$
0	–16	0
5	–21.2	0
7	–22.772	0
10	–26.5	0

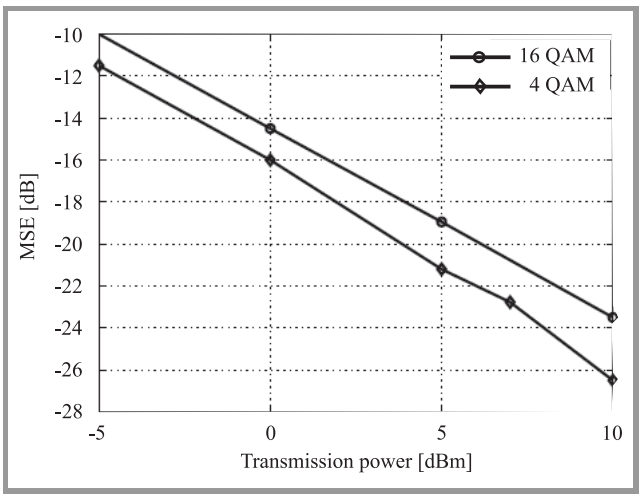

Fig. 10. The measured MSE of the OFDM symbols versus the transmission power with modulation scheme 16 QAM and 4 QAM at distance ($d = 2$ m).

Figure 11 illustrates the measured MSE of the received OFDM symbols for 16 QAM at transmission power

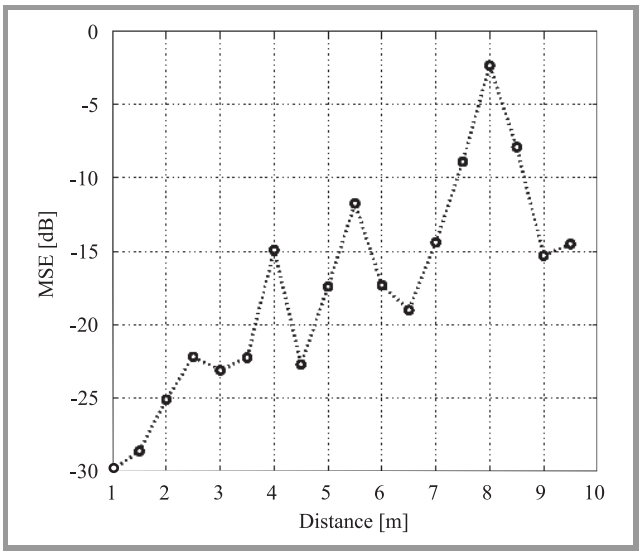

Fig. 11. The measured MSE of the OFDM symbols versus the distance between the transmitter and the receiver with modulation scheme 16 QAM and transmission power 17 dBm.

of 17 dBm and variant distance between the transmitter and the receiver. It can be seen from the figure that in addition to the path loss, the signal gets attenuated (shadowed) at certain distances because of the multipath effect.

5. Conclusion

This paper presents a method for estimating the wireless channel for OFDM system. A measurement system based on off-line measurement has been used for testing the OFDM signal. This system has been used to characterize the multipath channel and test the transmission, reception and channel estimation of the OFDM-based WLAN system. A method of joint channel and frequency offset estimation based on the signal preamble and Wiener filtering has been implemented. The measured results show that, combining the Wiener filtering and the autocorrelation can compensate for ICI and the phase rotations caused by frequency offsets and multipath effect.

Appendix

Calculating $\mathbf{R}$ and $\underline{\mathbf{P}}$

Assuming that $\mathbf{H}$, $\underline{\mathbf{S}}$, and $\underline{\mathbf{V}}$ are uncorrelated and making use of Eq. (4), the element (k,k') of $\mathbf{R}$ can be written as

$$\begin{aligned} R_{k,k'} &= E\{Y(k)Y(k')^*\} \\ &= E\Big\{\Big(\sum_{m=0}^{N-1} H_{m,k}S(m)\Big)\Big(\sum_{m'=0}^{N-1} H^*_{m',k'}S(m')^*\Big)\Big\} \\ &\quad + E\{V(k)V(k')^*\}. \end{aligned} \tag{21}$$

From Eq. (21), $\mathbf{R}$ can be separated into two parts, the pure correlation matrix and the noise

$$\mathbf{R} = \mathbf{R}' + \sigma_v^2\mathbf{I}, \tag{22}$$

where σ_v^2 is the noise variance, which is the first statistical parameter that needs to be estimated at the receiver. Also the element k' of $\underline{\mathbf{P}}_{m,k}$ is calculated as

$$\begin{aligned} P^{k'}_{m,k} &= E\{Y(k')H^*_{m,k}\} \\ &= E\Big\{\sum_{m'=0}^{N-1} H_{m',k'}H^*_{m,k}S(m')\Big\} \\ &\quad + E\{V(k')H^*_{m,k}\}. \end{aligned} \tag{23}$$

Assuming a wide sense stationary uncorrelated scattering (WSSUS) channel model, $R'_{k,k'}$ and $P^{k'}_{m,k}$ can be given by the following equations [22]:

$$\begin{aligned} R'_{k,k'} &= \sigma_s^2 \sum_{m\notin\underline{\mathbf{S}}_p} \sum_{l=0}^{L-1} \int_{-\infty}^{\infty} \Phi_{l,\mathrm{v}}(k-m,k'-m)d\mathrm{v} \\ &\quad + \sum_{m,m'\in\underline{\mathbf{S}}_p} S(m)S^*(m') \sum_{l=0}^{L-1} \mathrm{e}^{-\mathrm{j}2\pi(m-m')\Delta f\tau_l} \\ &\quad \int_{-\infty}^{\infty} \Phi_{l,\mathrm{v}}(k-m',k'-m')d\mathrm{v}; \end{aligned} \tag{24}$$

$$\begin{aligned} P^{k'}_{m,k} &= \sum_{m'\in\underline{\mathbf{S}}_p} S(m') \sum_{l=0}^{L-1} \mathrm{e}^{-\mathrm{j}2\pi(m-m')\Delta f\tau_l} \\ &\quad \int_{-\infty}^{\infty} \Phi_{l,\mathrm{v}}(k'-m',k-m)d\mathrm{v}, \end{aligned} \tag{25}$$

where

$$\Phi_{l,\mathrm{v}}(a,b) = \mathrm{sinc}(\mathrm{v}T_s - a)\,\mathrm{sinc}(\mathrm{v}T_s - b)D_l(\mathrm{v}),$$

where $\mathrm{sinc}(\cdot)$ is the sinc function and $D_l(\mathrm{v})$ is the Doppler spectrum for each tap. This term can be ignored in the case of time-invariant channels.

References

[1] C. Smith and J. Meyer, *3G Wireless with 802.16 and 802.11*. New York: McGraw-Hill, 2004.

[2] "Radio Broadcasting Systems; Digital Audio Broadcasting (DAB) to mobile, portable and fixed receivers", ETSI EN 300 401 V1.4.1, 2006.

[3] "Digital Video Broadcasting (DVB); Interaction channel for Digital Terrestrial Television (RCT) incorporating Multiple Access OFDM", ETSI EN 301 958 V1.1.1, 2002.

[4] P. Lescuyer and T. Lucidarme, *Evolved Packet System (EPS): The LTE and SAE Evolution of 3G UMTS*. Chichester: Wiley, 2008.

[5] S. Hara and R. Prasad, *Multicarrier Techniques for 4G Mobile Communications*. Boston, London: Artech House, 2003.

[6] J. Linartz and A. Grokhov, "New equalization approach for OFDM over dispersive and rapidly time varying channel", in *Proc. PIMRC 2000 Conf.*, London, UK, 2000.

[7] Y. Liao and K. Chen, "Estimation of stationary phase noise by the autocorrelation of the ICI weighting function in OFDM systems", *IEEE Trans. Wirel. Commun.*, vol. 5, no. 12, pp. 3370–3374, 2006.

[8] M. Chang, "A novel algorithm of interference self-cancellation for OFDM systems", *IEEE Trans. Wirel. Commun.*, vol. 6, no. 8, pp. 2881–2893, 2007.

[9] W. Jeon, K. Chang, and Y. Cho, "An equalization technique for orthogonal frequency-division multiplexing systems in time-variant multipath channels", *IEEE Trans. Wiurel. Commun.*, vol. 47, no. 1, pp. 27–32, 1999.

[10] R. Nee and R. Prasad, *OFDM for Wireless Multimedia Communications*. Boston, London: Artech House, 2000.

[11] "Agilent N5182A MXG Vector Signal Generator", Agilent Technol., 2007, Data sheet, ftp://ftp.testequity.com/pdf/n5182a.pdf

[12] D. Mittelstrasz, "Design Einer Antenne Bestehend aus Primaerstrahler und Dielektrischer Linse fuer das ISM-Band 2.4 GHz", Studienarbeit: Otto-von-Guericke Universitaet Magdeburg, 2007.

[13] A. Bandyopadhyay, M. Anis, A. Joestingmeier, T. Meyer, and A. Omar, "Analysis of a compact ultra-wideband antenna for radio frequency applications", in *Proc. Antenn. Propag. Soc. Int. Symp.*, Honolulu, Hawaii, USA, 2007, vol. 9, pp. 1965–1968.

[14] "Agilent EXA Signal Analyzer N9010A", Agilent Technol., 2009, Data Sheet, http://cp.literature.agilent.com/litweb/pdf/5989-6529EN.pdf

[15] T. Rappaport, *Wireless Communications: Principles and Practice*. New York: Prentice Hall, 2001.

[16] J. Heiskala and J. Terry, *OFDM Wireless LANs: A Theoretical and Practical Guide*. New York: Sams, 2001.

[17] T. Schmidl and D. Cox, "Robust frequency and timing synchronization for OFDM", *IEEE Trans. Commun.*, vol. 45, no. 12, pp. 1613–1621, 1997.

[18] H. Van Trees, *Detection, Estimation, and Modulation Theory. Part I: Detection, Estimation, and Linear Modulation Theory*. New York: Wiley, 1968.

[19] H. Poor, *An Introduction to Signal Detection and Estimation*. Berlin: Springer, 1994.

[20] S. Kay, *Fundamentals of Statistical Processing*. Volume I: *Estimation Theory*. Signal Processing Series. Upper Saddle River: Prentice Hall, 1993.

[21] M. Barkat, *Signal Detection and Estimation*. Norwood: Artech House, 2005.

[22] C. Sgraja and J. Linder, "Estimation of rapid time-variant channels for OFDM using wiener filtering", *IEEE Proc. Commun.*, vol. 4, pp. 2390–2395, May 2003.

Ali Ramadan Ali received the B.Sc. degree in electrical engineering from Altahadi Universiy, Sirt, Libya, in 1997 and the M.Sc. degree in electrical engineering from Darmstadt University of Applied Science, Germany, in 2004. He works toward the Ph.D. degree at the Otto-von-Guericke University of Magdeburg, Germany. His current research field covers the areas of digital signal processing for OFDM systems and microwave filter design. He authored or co-authored over 23 technical papers in the field of wireless communications and microwave filters.
e-mail: ali.ramadan@ovgu.de
Otto-von-Guericke University of Magdeburg
Institute for Electronic, Signal Processing
and Communications (IESK)
Chair of Microwave and Communication Engineering (HF)
P.O. Box 4120
Universitaetsplatz 2
39016 Magdeburg, Germany

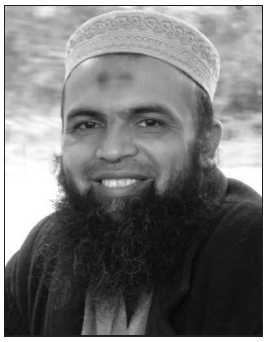

Tariq Jamil Khanzada received the M.Eng. degree in communication systems and networking, and B.Eng. degree in computer systems from Mehran University of Engineering and Technology (MUET), Pakistan, in 2004 and 1999, respectively. He currently works at the Institute of Electronics, Signal Processing and Communications (IESK), Otto-von-Guericke University of Magdeburg, Germany, since June 2005 in order to pursue his Ph.D. degree. Prior to start his Ph.D. studies he has been working as an Assistant Professor at the Department of Computer Systems and Software Engineering at MUET, since 2004 and as a lecturer since 2001. He is also a co-author of a practical book on computer workshop published in 2004. He is also an author of some international research publications.
e-mail: Tariq.Khanzada@ovgu.de
Otto-von-Guericke University of Magdeburg
Institute for Electronic, Signal Processing
and Communications (IESK)
Chair of Microwave and Communication Engineering (HF)
P.O. Box 4120
Universitaetsplatz 2
39016 Magdeburg, Germany

Abbas Omar received the B.Sc. and M.Sc. degrees in electrical engineering from Ain Shams University, Cairo, Egypt, in 1978 and 1982, respectively, and the Ph.D. degree in electrical engineering from the Technical University of Hamburg, Germany, in 1986. Since 1990, he has been a Professor of electrical engineering, and since 1998, a Director of the chair of microwave and communication engineering with Otto-von-Guericke University of Magdeburg, Germany. He authored or co-authored over 250 technical papers extending over a wide spectrum of research areas. His current research fields cover the areas of microwave, nuclear magnetic resonance, and ultrasonic imaging, remote sensing, microwave measurements, indoor and outdoor positioning systems, wideband wireless (terrestrial and mobile) communication, subsurface tomography and ground penetrating radar, ultra-wideband antennas, and field theoretical modeling of microwave systems and components. He is a member of the Editorial Board of some international technical periodicals.
e-mail: a.omar@ieee.org
Otto-von-Guericke University of Magdeburg
Institute for Electronic, Signal Processing
and Communications (IESK)
Chair of Microwave and Communication Engineering (HF)
P.O. Box 4120
Universitaetsplatz 2
39016 Magdeburg, Germany